

Charmonium, Bottomonium, B_c Mesons from Classical Pure SU(3) Yang-Mills Configurations

O. Oliveira*, R. A. Coimbra†

Centro de Física Computacional, Departamento de Física,
Universidade de Coimbra, 3004-516 Coimbra, Portugal

December 2, 2024

Abstract

A generalized Faddeev-Niemi ansatz for the gluon field is discussed. In its simplest parametrization, the ansatz allows a solution of the classical SU(3) Yang-Mills equations and from these solutions a confining potential for heavy quarkonia is defined. The investigation of charmonium and bottomonium proves that the potential is able to reproduce the spectra at the level of 3% for charmonium and 1% for bottomonium. Moreover, for charmonium the results for the semileptonic widths are in line with the other quark model calculations. For bottomonium, the semileptonic widths show good agreement with the recent CLEO measurements. The B_c spectra is also investigated.

1 Introduction and motivation

Quantum Chromodynamics (QCD) describes the interaction between quarks and gluons. QCD is a non-abelian gauge theory and besides the quark-gluon interaction it includes gluon-gluon interactions. It is expected that these interactions are responsible for the usual baryons and mesons together with exotic states like, for example, glueballs and gluelumps. In QCD, the basic building blocks are the quark and gluon fields. However, it appears that nature has a preference for baryons and meson states, i.e. colour singlet states, rather than single isolated quarks or exotic states. It seems that quarks are confined within hadrons. The theory provides hints about the mechanism which confines quarks within hadrons, but a fully explanation for confinement is still lacking.

The simplest picture suggesting quark confinement is the singlet potential computed from Wilson loops [1, 2, 3, 4]. This potential can be viewed as the energy between two static colour charges. For large quark separations, the

*email: orlando@teor.fis.uc.pt

†email: rita@teor.fis.uc.pt

potential grows linearly making it impossible to separate the quarks. In this sense, the singlet potential is a confinement mechanism applicable to heavy quarks. For light quarks, even the idea of describing the quark-quark interaction via a non-relativistic potential is questionable.

Besides the Wilson singlet potential, two popular confinement mechanisms are the dual Meissner effect [5, 6, 7, 8] and the vortex condensation picture [9, 10, 11, 12, 13]. In both pictures, confinement is explained invoking special types of gluon configurations, namely the condensation of magnetic monopoles in the dual picture and the percolation of colour vortices in the condensation case. Although, a considerable amount of work has been done in both scenarios, their precise confirmation is still missing.

The above described scenarios do not exhaust possible explanations for quark confinement. Many other mechanisms can be found in the literature. Typically, these mechanisms look for certain types of gluon configuration which, in principle, explain why we are not able to detect a free quark. Implicitly, they assume that the origin of confinement is within the pure gauge sector. The success of the quenched approximation in lattice QCD further supports such an idea.

The interaction between heavy quarks (charm/bottom hadrons) can be studied with non-relativistic quark models [14]. Hopefully, the interquark potential [15, 16, 17, 18, 19] should be derived from QCD. In practice, the potentials are either phenomenological or, at best, QCD-motivated. The idea of defining an interquark potential is appealing and, if one could solve the theory, the potential should be related to a given gluon configuration as in QED. So far, the known solutions of the classical field $SU(3)$ gauge theory, i.e. instantons, do not suggest quark confinement.

In this paper we construct solutions of the classical field $SU(3)$ Yang-Mills theory, in Minkowsky spacetime, which lead to confining nonrelativistic potentials¹. The classical solutions are obtained after the introduction of a generalized Cho-Faddeev-Niemi-Shabanov ansatz which, in Landau gauge, allows a parametrization of the gluon field in terms of two vector fields and a scalar field. For such a gluonic field, the classical field equations are essentially a system of coupled QED like equations for the two vector fields and a massless Klein-Gordon equation for the scalar field. The solutions of the coupled equations can be divided into QED like solutions, i.e. plane wave solutions, and exponential growing fields. The later ones will be identified with confining potentials. Although the potential is given by a multipole expansion, in this work only the $l = 0$ term will be considered. In order to compute its parameters, the potential is compared with the singlet potential computed from the Wilson loop. It comes that, in the range 0.2 - 1 fm, the new potential follows closely the Wilson loop behaviour, with a maximum deviation of about 50 MeV. The differences being both the small ($\mathcal{O}(1/r)$) and large ($\mathcal{O}(\exp(\Lambda r)/r)$) distance behaviours. Moreover, the potential is characterized by a single mass scale $\Lambda = 228$ MeV, computed together with the other parameters by fitting the singlet potential in the region 0.2 - 1 fm. Being close to the singlet potential, the charmonium,

¹See [20, 21] for related work.

bottomonium and $b\bar{c}$ spectrum is well described by the new potential. For charmonium, including spin-dependent forces, the difference between the theoretical predictions and experimental figures is below 2-3%. For bottomonium, this difference is reduced to 1% or less. However, in the semileptonic decays, the decay widths computed with the new potential are much closer and in good agreement with the experimental figures.

The paper is organized as follows, in section 2, for completeness, the generalized Cho-Faddeev-Niemi-Shabanov ansatz proposed previously is discussed, giving particular attention to its simplest parametrization. In section 3, a potential is built and compared with the singlet potential computed from the Wilson loop. The potential parameters are calculated fitting the singlet potential in the region 0.2 - 1 fm. In section 4, the charmonium, bottomonium and B_c spectrum is computed with the new potential, including the effect of spin-dependent forces. The recently discovered charmonium states and their possible quantum numbers assignment are discussed. Furthermore, discussion of the hadronic decays and semileptonic decays of the 1^{--} is performed. Finally, we draw the conclusions and plans for future work in the last section.

2 Classical Gluon Fields

For SU(3) the lagrangian density² reads

$$\mathcal{L} = -\frac{1}{4} F_{\mu\nu}^a F^{a\mu\nu} \quad (1)$$

where

$$F_{\mu\nu}^a = \partial_\mu A_\nu^a - \partial_\nu A_\mu^a - gf_{abc}A_\mu^b A_\nu^c, \quad (2)$$

and A_μ^a are the gluon fields. The classical equations of motion,

$$\partial_\mu F^{\mu\nu} + ig[A_\mu, F^{\mu\nu}] = 0, \quad (3)$$

being a set of non-linear partial differential equations are quite difficult to solve and to compute a solution of (3) it is usual to introduce an ansatz.

Following a procedure suggest in [23], let us consider a real covariant constant field n^a . From its definition, it follows

$$D_\mu n^a = \partial_\mu n^a + ig(F^c)_{ab}A_\mu^c n^b = 0, \quad (4)$$

where F^a are the generators of representation to which n belongs. If one wants to parametrize the gluon field in terms of n , the scalar field should have, at least, as many color components as A_μ . The adjoint representation fullfils such condition and it will be assumed that n belongs to this representation, then

$$(F^b)_{ac} = -if_{bac}, \quad (5)$$

$$D_\mu n^a = \partial_\mu n^a + gf_{abc}n^b A_\mu^c = 0. \quad (6)$$

²In this work we use the notation of [22].

Multiplying the last equation by n^a it follows

$$\partial_\mu (n^a n^a) = 0. \quad (7)$$

From now on it will be assumed that $n^a n^a = 1$.

Defining the color projected field

$$C_\mu = n^a A_\mu^a \quad (8)$$

one writes the gluon field as

$$A_\mu^a = n^a C_\mu + X_\mu^a, \quad (9)$$

where X is orthogonal to n in the sense

$$n^a X_\mu^a = 0. \quad (10)$$

In order to establish the gauge transformation properties of the various fields, we consider infinitesimal gauge transformations,

$$U(x) = e^{-i\omega(x)} = 1 - i\omega(x) \quad (11)$$

$$\delta A_\mu^a = \frac{1}{g} \partial_\mu \omega^a + f_{abc} \omega^b A_\mu^c \quad (12)$$

$$\delta n^a = f_{abc} \omega^b n^c. \quad (13)$$

For C_μ , the transformation rule looks like a “projected abelian” gauge transformation

$$\delta C_\mu = \frac{1}{g} n^a \partial_\mu \omega^a. \quad (14)$$

For X_μ^a , the transformation property is non-linear in the field n . It follows from (9), (12) and (13)

$$\delta X_\mu^a = \frac{1}{g} (\delta^{ab} - n^a n^b) \partial_\mu \omega^b + f_{abc} \omega^b X_\mu^c \quad (15)$$

and

$$\delta (n^a X_\mu^a) = 0. \quad (16)$$

In order to build an usefull ansatz, one can go back to equation (6), replace the gluon field by the decomposition (9), multiply by $f_{ade} n^e$ and try to solve for the X field. After some algebra we get

$$f_{abc} n^b \partial_\mu n^c - \frac{2}{3} g X_\mu^a - g (d_{abe} d_{dce} - d_{dbe} d_{ace}) X_\mu^b n^c n^d = 0 \quad (17)$$

after using the SU(3) relation

$$f_{abc} f_{dec} = \frac{2}{3} (\delta_{ad} \delta_{be} - \delta_{ae} \delta_{bd}) + (d_{adc} d_{bec} - d_{bdc} d_{aec}), \quad (18)$$

where

$$d_{abc} = \frac{1}{4} \text{Tr} (\lambda^a \{ \lambda^b, \lambda^c \}) \quad (19)$$

and λ^a are the SU(3) Gell-Mann matrices. Equation (17) allows us to write

$$X_\mu^a = \frac{3}{2g} f_{abc} n^b \partial_\mu n^c + Y_\mu^a \quad (20)$$

and

$$n^a X_\mu^a = n^a Y_\mu^a = 0. \quad (21)$$

The first term of X_μ^a is a generalized Faddeev-Niemi ansatz [24]. The simplest non-trivial n field with norm one can be parametrized as

$$n^a = \delta^{a1} \sin \theta + \delta^{a2} \cos \theta. \quad (22)$$

Then, with the above definitions equation (17) implies the following relations between the Y fields

$$Y_\mu^2 = Y_\mu^1 \cot \theta, \quad (23)$$

$$Y_\mu^3 = \frac{1}{2g} \partial_\mu \theta, \quad (24)$$

$$Y_\mu^4 = Y_\mu^5 = Y_\mu^6 = Y_\mu^7 = 0, \quad (25)$$

which together with the color space orthogonality condition (21) gives the gluon field

$$A_\mu^a = n^a C_\mu - \frac{\delta^{a3}}{g} \partial_\mu \theta + \delta^{a8} B_\mu; \quad (26)$$

in the last equation we defined $B_\mu = Y_\mu^8$. The corresponding gluon field tensor components are

$$F_{\mu\nu}^a = n^a C_{\mu\nu} + \delta^{a8} B_{\mu\nu}, \quad (27)$$

where

$$C_{\mu\nu} = \partial_\mu C_\nu - \partial_\nu C_\mu, \quad B_{\mu\nu} = \partial_\mu B_\nu - \partial_\nu B_\mu. \quad (28)$$

For the above gluonic configuration, the classical action is a functional of the vector fields C_μ and B_μ ,

$$\mathcal{L} = -\frac{1}{4} (\mathcal{C}^2 + \mathcal{B}^2), \quad (29)$$

and the classical equations of motion (3) become QED-like equations

$$\partial^\mu C_{\mu\nu} = 0, \quad \partial^\mu B_{\mu\nu} = 0. \quad (30)$$

Moreover, the hamiltonian density and the spin tensor are given by the sum of the contributions of two abelian-like theories associated with C_μ and B_μ fields.

Note that the pure gauge theory at the classical level, is independent of θ . However, the inclusion of fermions implies a coupling θ -fermions. The coupling with θ is associated with the first three Gell-Mann matrices and, for configurations with $C_\mu = B_\mu = 0$ requires only λ^3 ; no coupling with the third color component and the coupling to the first two color components have opposite signs.

The computation of classical solutions of the equations for the gluon configuration considered requires gauge fixing. For the Landau gauge³, the full set of equations is

$$\partial^\mu C_\mu = 0, \quad \partial^\mu B_\mu = 0, \quad (31)$$

$$\partial^\mu \theta C_\mu = 0, \quad \partial^\mu \partial_\mu \theta = 0. \quad (32)$$

These together with the classical field equations have plane wave solutions characterized by a four momenta k such that $k^2 = 0$, the fields C_μ and B_μ are polarized perpendicularly to k ,

$$C_\mu(k, \lambda) = \epsilon_C(k, \lambda) e^{-ikx}, \quad k^\mu \epsilon_C(k, \lambda) = 0, \quad (33)$$

$$B_\mu(k, \lambda) = \epsilon_B(k, \lambda) e^{-ikx}, \quad k^\mu \epsilon_B(k, \lambda) = 0, \quad (34)$$

$$\theta(k) = \theta_0 e^{-ikx}, \quad (35)$$

and the third color component being polarized along k . Our aim is to identify possible solutions of the classical field equations (31), (32), (30) which can suggest confining solutions. We will not proceed with the discussion of the solutions of the above set of coupled equations but, instead, discuss a particular class of solutions.

For the pure gauge theory, the condition for a finite action/energy solution does not constraint θ . Let us consider the simplest non-trivial configuration one could think of, namely $C_\mu = B_\mu = 0$. This particular configuration has zero energy and the field equations are reduced to a massless Klein-Gordon equation for θ which can be solved by the usual separation of variables. Indeed, writing $\theta(t, \vec{r}) = T(t)V(\vec{r})$, it comes

$$\frac{T''(t)}{T(t)} = \frac{\nabla^2 V(\vec{r})}{V(\vec{r})} = \Lambda^2, \quad (36)$$

where Λ is mass scale which is invariant under rescaling of the gluon field. The solutions with $\Lambda^2 < 0$ are the usual free field solutions. For $\Lambda = 0$, the gluon field is linear in time and the spatial part is the usual solution of the Laplace equation. If $\Lambda^2 > 0$,

$$T(t) = A_T e^{\Lambda t} + B_T e^{-\Lambda t} \quad (37)$$

and writing

$$V(\vec{r}) = \sum_{l,m} V_l(r) Y_{lm}(\Omega) \quad (38)$$

³For the Coulomb gauge, the first two equations are slightly more complicated but in the third and fourth equation one should replace ∂ by ∇ , together with other obvious modifications.

where $Y_{lm}(\Omega)$ are the spherical harmonics, the functions $V_l(r)$ can be written in terms of the modified spherical Bessel functions of the 1st $I_{l+1/2}(z)$ and 3rd $K_{l+1/2}(z)$ kind, where $z = \Lambda r$,

$$V_l(r) = A_{lm} \frac{I_{l+1/2}(z)}{\sqrt{z}} + B_{lm} \frac{K_{l+1/2}(z)}{\sqrt{z}}. \quad (39)$$

These solutions have the same scale for the temporal and spatial parts and, asymptotically, are real exponential functions. For example, the lowest multipole solution is

$$V_0(r) = A \frac{\sinh(\Lambda r)}{r} + B \frac{e^{-\Lambda r}}{r} \quad (40)$$

and the associated gluon field is

$$A_0^3 = \Lambda (e^{\Lambda t} - b_T e^{-\Lambda t}) V_0(r), \quad (41)$$

$$\vec{A}^3 = -(e^{\Lambda t} + b_T e^{-\Lambda t}) \nabla V_0(r). \quad (42)$$

From equations (37), (38), (39) and as long as one can assume that quarks do not exchange energy and/or the mean life time of the particle is such $\Lambda t \ll 1$, one can build a potential to describe non-relativistic quark systems. If these conditions are applicable, one can view the spatial part of A_0^3 as a non-relativistic potential. In general, the non-relativistic potential is not spherical symmetric. However, if only the lowest multipole (40) is considered, one is back to the central potential picture.

3 A Non-relativistic Potential for Heavy Quarkonium

The coupling of the classical field configuration discussed in the previous section to the fermion fields requires the λ^3 Gell-Mann matrix, i.e.

$$\gamma^\mu \frac{\lambda^3}{2} \partial_\mu \theta \psi; \quad (43)$$

ψ should be understood as a quark Dirac spinor. Assuming that it makes sense to describe the heavy fermion interaction via a potential derived from the above gluon configuration, from the structure of λ^3 one naively expects a bound state, let us say the first color component, an unbound state, the second color component and a free particle solution, the third color component. Of course, the usual quark model picture for hadrons is recovered only after gauge transforming all fields. From now on, we will assume that the confining potential for heavy quarkonium is given by the lowest multipole of the spatial part of A_0^3 (40) and that the Schrödinger equation for heavy mesons is, in first approximation,

$$\left\{ -\frac{\nabla^2}{2m} + V_0(r) \right\} \phi = i \partial_t \phi \quad (44)$$

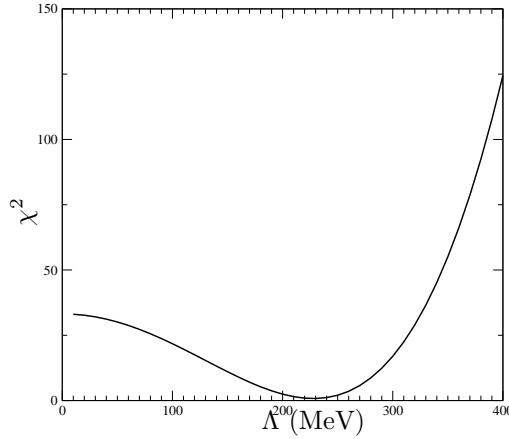


Figure 1: Minima of χ^2 as function of Λ .

where ϕ is a heavy meson field and m the reduced mass of the quarkonium system. Then, for small quark distances, the potential (40) is coulombic

$$V_0(r) = \frac{B}{r}, \quad (45)$$

and for large distances is confining

$$V_0(r) = \frac{A}{2r} e^{\Lambda r}. \quad (46)$$

For large inter-quark distances, the wave function goes to zero as

$$\phi(\vec{r}) \longrightarrow \frac{1}{r} \exp \left\{ -\frac{2}{\Lambda} \sqrt{\frac{mA}{r}} \exp \left[\frac{\Lambda r}{2} \right] \right\}, \quad \text{for } r \gg 1, \quad (47)$$

with the spatial extension of the quark field becoming smaller for heavier quarks.

The first step towards a proper definition of V_0 as a potential for heavy quark systems is the computation of its various parameters, namely A , B and Λ . This can be done by minimizing the square difference between the new potential and the singlet potential computed from Wilson loops. For the singlet potential we used the results from [3] at $\beta = 6.4$. The

$$\chi^2 = \int_{r=0.2fm}^{r=1fm} dr \left[V_0(r) - V_{singlet}(r) \right]^2 \quad (48)$$

as function of Λ can be seen in figure 1. The curve shows an absolute minimum and we take the potential parameters as their values at this point,

$$A = 11.2542671, \quad B = -0.70113530875, \quad \Lambda = 228.026 \text{ MeV} \quad (49)$$

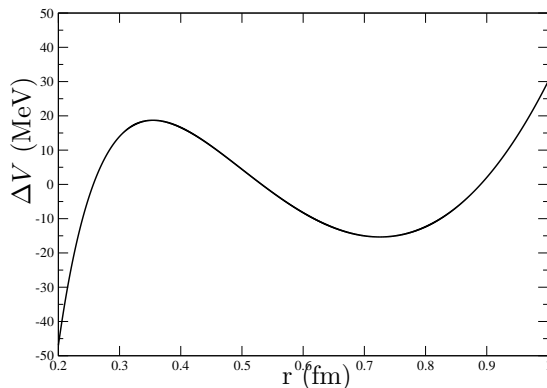


Figure 2: $\Delta V = V_0(r) - V_{singlet}(r)$.

when r is measured in MeV^{-1} . The difference between V_0 and the lattice potential is reported in figure 2.

It is curious that the value of the only energy scale in the solution is close to standard values for Λ_{QCD} . We have no interpretation for this result. Probably, it is connected to the way the parameters are defined, i.e. to the fit of V_0 to the lattice singlet potential.

Assuming that the short distance behaviour of the inter-quark potential is dominated by the one-gluon exchange contribution, then $B = -4\alpha_s/3$ and the strong coupling constant associated to the above value for B is $\alpha_s = 0.526$. This value is about twice the value defined for α_s from the spin-dependent forces used in the spectrum calculation - see table 2 below.

4 Heavy quark mesons: charmonium, B_c , bottomonium

The potential $V_0(r)$ is a first approximation to the full interaction. From the various possible corrections, it will be assumed that the spin dependent part gives the dominant contribution. Hopefully, the spin dependent can be computed perturbatively as in [25], where the spin dependent potential was written as

$$V_1 = \sum_{k=1}^4 T_k, \quad (50)$$

with

$$T_1 = \frac{\vec{L} \cdot \vec{s}_i}{2m_i^2} \bar{T}_1(m_i, m_j) + \frac{\vec{L} \cdot \vec{s}_j}{2m_j^2} \bar{T}_1(m_j, m_i), \quad (51)$$

$$T_2 = \frac{\vec{L} \cdot \vec{s}_i}{m_i m_j} \bar{T}_2(m_i, m_j) + \frac{\vec{L} \cdot \vec{s}_j}{m_i m_j} \bar{T}_2(m_j, m_i), \quad (52)$$

$$T_3 = \frac{\vec{s}_i \cdot \vec{s}_j}{m_i m_j} \bar{T}_3(m_i, m_j), \quad (53)$$

$$T_4 = \frac{S_{ij}}{m_i m_j} \bar{T}_4(m_i, m_j), \quad (54)$$

where \vec{L} is the orbital angular momentum, \vec{s}_i the spin of the quark i , m_i its mass and

$$S_{ij} = 4 \left[3 (\vec{s}_i \cdot \hat{r}) (\vec{s}_j \cdot \hat{r}) - \vec{s}_i \cdot \vec{s}_j \right] \quad (55)$$

is the tensor operator. The various T_k where computed in perturbation theory assuming that the magnetic interactions are short range (see [25]),

$$\bar{T}_1(m_i, m_j) = - \left\langle \frac{1}{r} \frac{dV_0}{dr} \right\rangle + 2 \bar{T}_2(m_i, m_j), \quad (56)$$

$$\bar{T}_2(m_i, m_j) = \frac{4\alpha_s}{3} \langle r^{-3} \rangle, \quad (57)$$

$$\bar{T}_3(m_i, m_j) = \frac{32\pi\alpha_s}{9} |\Psi(0)|^2, \quad (58)$$

$$\bar{T}_4(m_i, m_j) = \frac{\alpha_s}{3} \langle r^{-3} \rangle; \quad (59)$$

$$(60)$$

$\Psi(0)$ is the meson wave function at the origin. With the above definitions, the potential verifies the Gromes constraint [26] that arises from the boost invariance of the QCD.

In the following, the particles are classified according to the usual spectroscopic notation $n^{2S+1}L_J$, where S is the total spin and J the total angular momenta. The Schrödinger equation is solved for $V_0(r)$ with the wave function $\Psi_{nlm}(\vec{r}) = R_{nl}(r) Y_{lm}(\theta, \phi)$, where n is the principal quantum number, l and m are the orbital angular momentum and its projection, $R_{nl}(r)$ is the radial wave function and $Y_{lm}(\theta, \phi)$ are the spherical harmonic functions. We further define

$$R_{nl}^{(l)}(0) = \frac{d^l R_{nl}(0)}{dr^l}, \quad (61)$$

i.e. the radial wave function and its derivatives at the origin. The various $R_{nl}^{(l)}(0)$ are required to compute production rates and decays rates. The total wave function is then built by coupling $\Psi_{nlm}(\vec{r})$ with the spin wave function.

4.1 Quark masses

The quark masses were adjusted to reproduce the charmonium and bottomonium $2S - 1S$ mass differences. According to our description, the mass of S wave mesons is given by

$$M(^1S_0) = m_0 - \frac{3}{4} \delta_{spin}, \quad M(^3S_1) = m_0 + \frac{1}{4} \delta_{spin}, \quad (62)$$

charmonium		bottomonium	
$\eta_c(1S)$	$J/\psi(1S)$	$\eta_b(1S)$	$\Upsilon(1S)$
2980.4 ± 1.2	3096.916 ± 0.011	$9300 \pm 20 \pm 20$	9460.30 ± 0.26
$\eta_c(2S)$	$\psi(2S)$	$\eta_b(2S)$	$\Upsilon(2S)$
3638 ± 5	3686.093 ± 0.034	—	10023.26 ± 0.31

Table 1: Meson masses, in MeV, used to define the quark mass. The particles masses are the particle data book values [27].

for spin zero and spin one particles, respectively; m_0 is the contribution due to the central potential and quark masses and δ_{spin} is the spin-spin splitting. Then, it follows that

$$m_0 = \frac{3}{4}M(^3S_1) + \frac{1}{4}M(^1S_0). \quad (63)$$

With the mesons masses reported in table 1 and adding the errors in quadrature,

$$m_0(c\bar{c}; 1S) = 3067.79 \pm 0.30 \text{ MeV}, \quad \delta_{spin}(c\bar{c}; 1S) = 116.5 \pm 1.2 \text{ MeV}. \quad (64)$$

$$m_0(c\bar{c}; 2S) = 3674.1 \pm 1.2 \text{ MeV}, \quad \delta_{spin}(c\bar{c}; 2S) = 48.1 \pm 5.0 \text{ MeV}. \quad (65)$$

$$m_0(b\bar{b}; 1S) = 9420.2 \pm 7.0 \text{ MeV}, \quad \delta_{spin}(b\bar{b}; 1S) = 160 \pm 28 \text{ MeV}, \quad (66)$$

and

$$\Delta M(c\bar{c}) = m_0(c\bar{c}; 2S) - m_0(c\bar{c}; 1S) = 606.3 \pm 1.2 \text{ MeV}, \quad (67)$$

$$m_0(b\bar{b}; 2S) - m_0(b\bar{b}; 1S) = 603.1 \pm 7.0 \text{ MeV} \quad (68)$$

where for the bottomonium spectrum we used only the information from the $J^{PC} = 1^{--}$ state $\Upsilon(2S)$.

The $J^{PC} = 0^{-+}$ bottomonium spectrum is not as wellknown as the charmonium. The experimental mass of $\eta_b(1S)$ has large errors and there is no experimental information on $\eta_b(2S)$. Then, for the bottomonium, we decided to replace the mass splitting (68) by the value obtained using directly the 1^{--} states

$$\Delta M(b\bar{b}) = M(\Upsilon(2S)) - M(\Upsilon(1S)) = 562.96 \pm 0.40 \text{ MeV}. \quad (69)$$

The motivation being the following. If one assume that the spin splitting scales as

$$\frac{\delta_{spin}(c\bar{c})}{\delta_{spin}(b\bar{b})} = \frac{m_b^2}{m_c^2}, \quad (70)$$

the $\delta_{spin}(b\bar{b})$ can be computed using $\delta_{spin}(c\bar{c})$ and the central values for the quark masses given in [27]. m_0 can be obtained from the $\Upsilon(1S)$ value by subtracting the spin contribution giving $m_0 = 9457.8 \text{ MeV}$, a figure close to the $\Upsilon(1S)$ mass. Moreover, for the charmonium the $2S$ spin splitting is $\sim 48 \text{ MeV}$. Again, we expect a similar scaling law relating the splittings for the $2S$ states. This

	V_0	QCD(BT)	$ R_{nl}^{(l)}(0) ^2$	Power law	Logarithmic	Cornell
1S	0.979	0.810	0.999	0.815	1.454	
2S	0.841	0.529	0.559	0.418	0.927	
3S	0.892	0.455	0.410	0.286	0.791	
2P	0.145	0.075	0.125	0.078	0.131	
3P	0.240	0.102	0.131	0.076	0.186	
3D	0.122	0.015	0.026	0.012	0.031	
α_s	0.2718(28)	0.3544(37)	0.4251(44)	0.3618(37)	0.3052(31)	

Table 2: Charmonium radial wave function and its derivatives at the origin. All quantities are in GeV^{2l+3} . The first column reports the value computed using $V_0(r)$ and all others are taken from [28]. The references for the various potentials are: QCD(BT) [16], Power law [17], Logarithmic [18], Cornell [19]. For the definition of the strong coupling constant α_s see text below.

gives $\delta_{spin}(bb) = 4 \text{ MeV}$. One can estimate an error in the spin splitting by adding, in quadrature, the errors in (62) giving 3 MeV , i.e. a value which is half of the figure in (68).

Adjusting the quark masses to reproduce the mass differences (67) and (69) up to the MeV scale gives

$$m_c = 1425 \text{ MeV}, \quad m_b = 4194.5 \text{ MeV} \quad (71)$$

which are within typical values.

4.2 Charmonium

The charmonium radial wave function and its derivatives, for various states, are reported and compared with other quark model calculations in table 2.

For S wave mesons and for V_0 , the wave function at the origin is essentially constant. For the other potentials and for the states reported in table 2, $R(0)$ decreases when the principal quantum number increases. This is a major difference between V_0 and the other potentials. For V_0 this means that the decays widths which are sensible to the wave function at the origin, such as the semileptonic decays, should scale approximately with the inverse of meson mass squared. For the other potentials this scaling behaviour is not verified. Looking at $R(0)$, the potential which is closer to V_0 is the Cornell potential.

For P mesons, the first derivative of the wave function at the origin increases with the principal quantum number for the QCD inspired potentials V_0 , QCD(BT) and Cornell. The largest increase reported in table 2 happens for V_0 . For the other two potentials, $|R^{(1)}(0)|^2$ is essentially constant.

For the only D meson reported in table 2, V_0 shows a second derivative at the origin an order of magnitude larger than all other potentials. Thus, V_0 enhances, for example, the semileptonic decay of the D meson states when compared with all other models.

In order to compute the full spectrum, including the spin effects, a definition for the strong coupling constant is required. As α_s is sensible to the $1^3S_1 - 1^1S_0$ mass difference

$$\Delta M(1^3S_3 - 1^1S_1) = \frac{8}{9} \alpha_s \frac{|R_{10}(0)|^2}{m_c^2}, \quad (72)$$

the above relation was used to define the strong coupling constant. Its value for the various models is also reported in table 2. Note that V_0 produces the smallest α_s and that the figure is lower than the coupling reported in the particle data value for the charm mass used in this work, $\alpha_s(m_c) = 0.357_{-21}^{+23}$. Recently, the CLEO collaboration [29] was able to measure the strong coupling from the ratio $\Gamma(\chi_{c2} \rightarrow \gamma\gamma)/\Gamma(\chi_{c2} \rightarrow gg)$. The experimental number, $\alpha_s = 0.29 \pm 0.01$, is in good agreement (up to two standard deviations) with V_0 and Cornell potential estimates.

Setting $m_c = 1.425$ GeV and $\alpha_s = 0.2718$ the charmonium spectrum was computed evaluating the spin effects in perturbation theory. In table 3 the full spectrum is reported taking

$$M(\text{meson}) = 2m_c + E_{NR} + \Delta_{cc}, \quad (73)$$

where E_{NR} is the eigenvalue of the Schrödinger equation and $\Delta_{cc} = -2451.8$ MeV is a shift introduced to reproduce the $1S$ experimental mass values. This mass shift, Δ_{cc} , can be viewed as a non-perturbative contribution which is not accessible within the model. In the following, it will be assumed that Δ_{cc} is the same within each quarkonium spectrum.

Table 3 shows the model predictions, together with experimental results, including the recently discovered charmonium states $X(3872)$ [30, 31], $Z(3930)$ [32], $X(3940)$ [33], $Y(4260)$ [34]. The experimental values are taken from [27] with the exception of the new states and the mesons reported below. For $h_c(1P)$ we quote the CLEO result [35]. For $\eta'(2S)$ we quote the combined value of the recent Belle, Babar and CLEO measurements [36, 37, 38, 39, 40] and not the larger mass of the particle data book, 3638 ± 5 MeV. For $\psi(3770)$ we use the result of the KEDR collaboration [41] reported at the HEP2005 conference.

On overall, one can find good agreement between the experimental numbers and the model predictions. Typically, the predictions are lower than the measured masses with deviations of the order of $2 - 3\%$. Since, there are various charmonium states whose quantum numbers have never been measured experimentally, in the following sections we comment on our results and possible quantum numbers assigns. The decays of the various charmonium states will be discussed in the next subsection.

4.2.1 $h_c(1P)$

The meson was observed by CLEO [35] and the Cristal Ball [42, 43] collaborations in the reaction

$$e^+e^- \longrightarrow \psi(2S) \longrightarrow \pi^0 h_c, \quad (74)$$

with $h_c \longrightarrow \gamma \eta_c(1S)$ and $\pi^0 \longrightarrow \gamma \gamma$ and by the E760 collaboration [44] in the reaction

$$p\bar{p} \longrightarrow h_c \longrightarrow \pi^0 J/\psi, \quad (75)$$

with $J/\psi \longrightarrow e^+e^-$. The production and decay of h_c favours $J^{PC} = 1^{++}$. In the model, the closest mass state with these quantum numbers being the 1^1P_1 state. The predicted mass deviates from the experimental value by 1.3%.

4.2.2 $\eta'_c(2S)$

The $\eta'_c(2S)$ was seen in the process

$$e^+e^- \longrightarrow (e^+e^-) \gamma \gamma, \quad (76)$$

via the two photon fusion [39, 40]

$$\gamma \gamma \longrightarrow \eta'_c \longrightarrow K_S K^\pm \pi^\pm, \quad (77)$$

and in the decays [37]

$$B^+ \longrightarrow K^+ \eta'_c(2S), \quad B^0 \longrightarrow K_S \eta'_c(2S), \quad \eta'_c(2S) \longrightarrow K_S K^- \pi^+. \quad (78)$$

Concerning the determination of the quantum numbers of $\eta'_c(2S)$, certain combinations have been excluded by experiment [40]. The allowed J^P are 0^- , 2^\pm , 3^+ , 4^\pm , \dots with $C = +$. Combining the measure mass and the information on the quantum numbers. it seems natural to identify $\eta'_c(2S)$ with the 2^1S_0 state. The model prediction differs from the experimental mass by 1.1%.

The various collaborations have published results for mass differences. Combining the errors in quadrature,

$$\begin{aligned} \Delta M(2S - 1S) = M(\eta'_c(2S)) - M(\eta_c(1S)) = & 661.1 \pm 3.9 \text{ MeV} \quad [39], \\ & 648.3 \pm 3.8 \text{ MeV} \quad [40], \\ & 675 \pm 6 \text{ MeV} \quad [37]. \end{aligned}$$

The error averaged combined result being

$$\Delta M(2S - 1S) = 659.57 \pm 0.59 \text{ MeV} \quad (79)$$

which differs from the model prediction 619 MeV by 6.6% giving further support to the above identification. However, in what concerns the hiperfine splitting $\Delta M_{hf}(2S) = M(\psi(2S)) - M(\eta'_c(2S))$ the model predicts a value of 100 MeV, roughly a factor of two higher than the latest measurements,

$$\begin{aligned} \Delta M_{hf}(2S) = M(\psi(2S)) - M(\eta'_c(2S)) = & 43.1 \pm 3.4 \text{ MeV} \quad [39], \\ & 55.2 \pm 4.0 \text{ MeV} \quad [40], \end{aligned}$$

the combined value⁴ being 48.67 ± 0.71 MeV. Note that our result is compatible with the early measurement of the Cristal Ball collaboration for the hiperfine splitting 92 ± 5 MeV [45]. For purposes of comparisation we quote the quenched lattice result for the splitting [46]: 34 ± 25 - 43 ± 29 MeV, depending on how the physical scale is chosen.

4.2.3 $\psi(3836)$

The experimental information on $\psi(3836)$ is scarce. Only two experiences [47, 48] have seen signs for this meson and, according to particle data book, $\psi(3836)$ still needs experimental confirmation. The measure of the quantum numbers of $\psi(3836)$ was discussed in [47]. Based on the comparisation with theoretical mass predictions, the authors suggest that it should be a 3D_2 state. Following the same reasoning, from the values of the mesons mass and considering the already excluded quantum numbers, within the calculation discussed here, this state can be identified with one of the 1^3D_3 , 1^3D_2 or 1^1D_2 states. For these states the mass difference between the prediction and the experimental figures are, respectively, 1.7%, 1.1% and 1.0%. Compared with the other mass values they are within the same level of precision.

4.2.4 $X(3872)$

This particle was discovered by Belle collaboration [49] in the decay $B^- \rightarrow X(3872)K^-$, with $X \rightarrow J/\psi\pi^+\pi^-$, and confirmed by CDF [50], D0 [51] and BABAR [52] collaborations. Experimentally, only the charge parity $C = +$ is well established with the data favouring [54, 55, 56] the assignment $J^{PC} = 1^{++}$. A $J^{PC} = 2^{++}$ is not ruled out but seems to be unlikely. In our calculation, the closest $C = +$ mass eigenstate being the 1^1D_2 state which shows a deviation from the experimental mass of 2.2%.

4.2.5 The 3940 MeV mass states

The Belle collaboration reported on the three possible new states with masses around 3940 MeV: $X(3940)$ [33], $Y(3940)$ [57] and $Z(3930)$ [32] with measured masses of $3943 \pm 11 \pm 13$ MeV, 3940 ± 11 MeV and 3931 ± 4 MeV, respectively. The $X(3940)$ was observed in the process $e^+e^- \rightarrow J/\psi X$, $Y(3940)$ was seen as a resonance in the decay $B \rightarrow K\pi\pi J/\psi$ and $Z(3930)$ was observed in the reaction $\gamma\gamma \rightarrow D^0\bar{D}^0$, D^-D^+ . For the Z particle, the helicity distribution of the final states particles favors a $J = 2$ assignment.

Looking at the mass values computed with the model under discussion, the natural candidates are the $2P$ and $1F$ levels. For Z , assuming that it has $J = 2$ and $C = +$, it should be a 2^3P_2 charmonium state. The theoretical computed mass shows a deviation from the experimental number of 2.7%. In what concerns the quantum numbers, for the remaining two states there is no experimental information. The decays of X and Y suggest that they should

⁴The combined value reported in [36] was 48.6 ± 4.4 MeV.

be associated with different levels. The closest mass states to the experimental measures are the available $2P$ levels. However, the decay patterns known so far do not match the pattern observed for the $1P$ states. Looking only at the mass values, a possible assignment being: 2^3P_0 for $Y(3940)$ (deviation of 1.5%) and 2^3P_1 for $X(3940)$ (deviation of 2.2%).

4.2.6 $Y(4260)$

This broad resonance was observed in $e^+e^- \rightarrow \gamma_{ISR}\pi^+\pi^-J/\psi$ with a mass of 4.26 GeV [34], meaning that it has the quantum numbers of the photon $J^{PC} = 1^{--}$. Of the levels in table 3 with these quantum numbers, the 3^3S_1 matches perfectly its mass. The deviation of the theoretical prediction to the experimental value being 0.3%.

4.2.7 $\psi(4040)$, $\psi(4160)$, $\psi(4415)$

The states $\psi(4040)$, $\psi(4160)$, $\psi(4415)$ were observed in $e^+e^- \rightarrow \text{hadrons}$ [60]. In what concerns its quantum numbers, there is no experimental information but it is usual to assume that they are vector particles. From table 3 and looking only to the mass values, there a number of states which can be associated with these particles within the 2% level of precision, i.e. to the following range of masses: 3918 – 4161 MeV for $\psi(4040)$; 4034 – 4284 MeV for $\psi(4160)$; 4283 – 4547 MeV for $\psi(4415)$. Given the lack of experimental information, hopefully, only after studying their production and decays will be possible to identify the associated quantum numbers.

4.2.8 Charmonium Decays

Charmonium decays can be investigated using the van Royen-Weisskopf [61] approach and including QCD corrections perturbatively. The computation of the decay widths requires only the knowledge of the wave function at the origin and its derivatives [62].

For S wave mesons, the following processes

$$\begin{aligned} n^3S_1 &\longrightarrow e^+e^-, \gamma\gamma\gamma, ggg, gg\gamma, \\ n^1S_0 &\longrightarrow \gamma\gamma, gg, \end{aligned}$$

will be considered, while for P wave mesons the decays

$$\begin{aligned} n^3P_2 &\longrightarrow \gamma\gamma, gg, \\ n^3P_1 &\longrightarrow q\bar{q}g, \\ n^3P_0 &\longrightarrow \gamma\gamma, gg \end{aligned}$$

will be computed. The values of $|R_{nl}^{(l)}(0)|^2$ from table 2 allow a comparison between the various heavy quarkonium potentials. For the mesons which have been measured experimentally, the predictions of the various models are compared in table 4:

- $\eta_c(1S)$ [1^1S_0]

The experimental value⁵ for the particle width is 25.5 ± 3.4 keV and $\Gamma(\gamma\gamma) = 7.0 \pm 1.0$ keV. In what concerns the total width, assuming that $\Gamma = \Gamma(\gamma\gamma) + \Gamma(gg)$, all quark models predictions are roughly a factor of two higher than the experimental figure. The model discussed in this paper gives 30.7 MeV, which deviates from the experimental number by less than two standard deviations.

In what concerns the radiative decay into photons, QCD(BT), the power law and the logarithmic potentials agree with the experimental numbers. V_0 deviates for the experimental figure by less than two standard deviations and the Cornell potential is far away from the measured value.

- $J/\psi(1S)$ [1^3S_1]

The experimental width is 91.0 ± 3.2 keV and recent measurements of the semileptonic width [66] give $\Gamma_{ee} = 5.68 \pm 0.11 \pm 0.11$ keV. In this article, the quoted total width being $95.5 \pm 2.4 \pm 2.3$ keV. The theoretical estimation of the width is given by $\Gamma(e^+e^-) + \Gamma(\mu^+\mu^-) + \Gamma(\gamma\gamma\gamma) + \Gamma(ggg) + \Gamma(gg\gamma)$. For all quark models, $\Gamma(\gamma\gamma\gamma)$ is of the order of a few eV without QCD corrections and, after QCD corrections, becomes negative. This behaviour is common to all S wave vector particles. Therefore, it will be assumed that the partial width $\Gamma(\gamma\gamma\gamma) \sim 0$.

All quark models overestimate the full width by a large factor, with the closest figure from V_0 ; roughly, a factor of two away of the experimental number.

The semileptonic decays of J/ψ into e^+e^- have been observed experimentally. According to the Particle Data Book $\Gamma(e^+e^-) = 5.40 \pm 0.15 \pm 0.07$ keV which agrees well with the result using V_0 . The Cornell potential overestimated the decay width and the remaining potentials underestimate the width by almost a factor of two.

- $\eta'_c(2S)$ [2^1S_0]

For this meson the particle data book quotes $\Gamma = 14 \pm 7$ MeV. The models predictions are 18 MeV (V_0), 21 MeV (QCD(BT)), 34 MeV (Power law), 18 (Logarithmic), 26 MeV (Cornell). The Cornell potential and the power law potential predictions are not compatible within one standard deviation with the PDG value.

On the two photon decay, the experimental limit⁶ obtained being $\Gamma(\gamma\gamma)/\Gamma < 0.01$ and the quark models predict branching ratios $\sim 10^{-6}$.

- $\psi(2S)$ [2^3S_1]

⁵In the following, the quoted experimental numbers are taken from the Particle Data Book [27], except when stated explicitly.

⁶The Particle Data Book quotes a $\Gamma(\gamma\gamma) = 1.3 \pm 0.6$ keV. However, the number was not a direct measurement but a derived value - see [27].

The measured particle width is 281 ± 17 keV. The quark model predictions being: 124 keV (V_0), 148 keV (QCD(BT)), 224 keV (Power law), 124 keV (Logarithmic), 186 keV (Cornell). The closest figure is associated with the power law potential. The QCD inspired models V_0 QCD(BT) and Cornell fail the experimental figure by a factor of roughly two.

The experimental measure of the semileptonic decays is 2.10 ± 0.12 keV for the partial width for the electronic decay. Recent measurements by CLEO [53] give $2.54 \pm 0.03 \pm 0.11$ keV. The closest prediction is from QCD(BT)⁷. The other quark models either overestimate (V_0 , Cornell) or underestimate (Power Law, Logarithmic) the measured width by roughly a factor of two.

Recently, the ratio $\Gamma_{ee}[\psi(2S)]/\Gamma_{ee}[J/\psi]$ was measured by CLEO [66]. The experimental number quoted in the paper is $0.45 \pm 0.01 \pm 0.02$. The various model predictions are: 0.60 (V_0), 0.46 (QCD(BT)), 0.40 (Power law), 0.36 (Logarithmic), 0.45 (Cornell). The closest figures are from the QCD(BT) and the Cornell potentials.

- $\psi(4040)$, $\psi(4160)$ [3^3S_1]

From the point of view of the meson masses, the best candidate for this state is the $\psi(4160)$. Its mass being of 4159 ± 20 MeV, a total width of 78 ± 20 MeV and a semileptonic width of 0.77 ± 0.23 keV. The corresponding values for $\psi(4040)$ are 4040 ± 10 MeV, 52 ± 10 MeV and 0.75 ± 0.15 keV.

The various theoretical predictions for the total width clearly underestimate by more than an order of magnitude the measured width. In what concerns the semileptonic width, the QCD inspired models (V_0 , QCD(BT), Cornell) overestimate the experimental number, with the remaining models underestimating it. At one standard deviation, the predictions of the power law and logarithmic potentials agree with $\psi(4040)$ and $\psi(4160)$ values. For $\psi(4160)$, QCD(BT) also agrees, within the same level of precision, with the experimental figure. The differences between all quark model predictions and the measured values for the various widths suggests that either the mesons are not pure 3^3S_1 states or their quantum numbers aren't those usually assumed.

In conclusion, for $J^{PC} = 0^{-+}$ mesons the power law and logarithmic potentials overestimate, by a large factor, the particles total widths. The QCD inspired models V_0 , QCD(BT), Cornell overestimate the total width, with V_0 being closer to the experimental number. In what concerns the two photon widths, it seems that the phenomenological potentials are closer to the experimental figures. Note, however, that the experimental width is in between the predictions of the QCD inspired models. For $J^{PC} = 1^{-+}$ the theoretical estimates deviate considerably from the experimental measures. For $J/\psi(1S)$, V_0 is able to predict the right semileptonic width but, in what concerns the total width, deviates by roughly a factor of two from the experimental number.

⁷However, if instead of the particle data book value, one considers the recent measured width, then V_0 and the Cornell potentials are closer to the experimental value.

The other quark models predict much larger widths than V_0 . For the remaining $J^{PC} = 1^{--}$, the situation is not so clear. In particular, in what concerns the total width, the predictions of the so called QCD inspired models are away from the experimental numbers, by one or two orders of magnitude. The semileptonic widths are of the same order of magnitude as the experimental figures but, again, the model numbers show large deviations, again roughly a factor of two. Probably, this is due to simple picture adopted here, suggesting that a coupled cluster analysis should be used instead of this central potential calculation with corrections.

Despite all limitations of the quark models, in table 5, the predictions of V_0 for the various processes considered are reported for charmonium.

The decay constant required to compute decay rates and production cross section for pseudoscalar mesons is defined by

$$\langle 0 | A_\mu(0) | M(p) \rangle = i f_M p_\mu, \quad (80)$$

where A_μ is the axial-vector current and p the four momenta of the meson M . Again, following the approach devised by van Royen-Weisskopf [61], the decay constant can be related to the wave function at the origin

$$f_M = \sqrt{\frac{3}{\pi M}} |R(0)|, \quad (81)$$

where M is the meson mass. Perturbative QCD corrections reduce f_M by a factor of $\sqrt{1 - 16\alpha_s/(3\pi)}$. Using the values reported in table 2 it comes, before QCD corrections,

$$f_{\eta(1S)} = \begin{cases} 560 \text{ MeV} & V_0, \\ 509 \text{ MeV} & \text{QCD(BT)}, \\ 566 \text{ MeV} & \text{Power Law}, \\ 511 \text{ MeV} & \text{Logarithmic}, \\ 683 \text{ MeV} & \text{Cornell.} \end{cases} \quad (82)$$

In the computation of pseudoscalar decay constant it was used the experimental measured mass.

4.2.9 Mixing Effects in Charmonium

For $J^{PC} = 1^{--}$ mesons, the semileptonic widths predictions from V_0 are reported in table 6. For $J/\psi(1S)$, the width is $0.86 \times \Gamma_{exp}$. For $\psi(2S)$ the model prediction is larger than the experimental number by a factor of 1.34. The prediction for $\psi(4040)$ and $\psi(3770)$ is far from the experimental value. The same applies to $\psi(4160)$ and $\psi(4415)$. The deviation can be explained, at least partially, in terms of mixing between states. In the model, the tensor interaction is responsible for the mixing of the central potential states. Indeed, $\psi(4040)$, $\psi(3770)$ and $\psi(4160)$, $\psi(4415)$ have the same spin and the same total spin. Moreover, the mass predictions for such states differ, within each of the group, by 100 MeV or less - see table 3. Despite the complete picture of the mixing

between the states being complex, one can estimate phenomenologically its relevance [67] for the two groups of $J^{PC} = 1^{--}$ states parametrizing each mixing via a single parameter

$$|\psi(3770)\rangle = \cos\theta |1^3D_1\rangle + \cos\theta |2^3S_1\rangle, \quad (83)$$

$$|\psi(2S)\rangle = -\sin\theta |1^3D_1\rangle + \cos\theta |2^3S_1\rangle, \quad (84)$$

and

$$|\psi(4415)\rangle = \cos\theta' |2^3D_1\rangle + \cos\theta' |3^3S_1\rangle, \quad (85)$$

$$|\psi(4160)\rangle = -\sin\theta' |2^3D_1\rangle + \cos\theta' |3^3S_1\rangle. \quad (86)$$

Then, the leptonic widths are given by [68]

$$\Gamma_{e^+e^-}(\psi(3770)) = \frac{4\alpha^2 e_c^2}{M^2[\psi(3770)]} \left| \sin\theta R_{2S}(0) + \frac{5}{2\sqrt{2}m_c^2} \cos\theta R_{1D}^{(2)}(0) \right|^2 \quad (87)$$

and

$$\Gamma_{e^+e^-}(\psi(2S)) = \frac{4\alpha^2 e_c^2}{M^2[\psi(2S)]} \left| \cos\theta R_{2S}(0) - \frac{5}{2\sqrt{2}m_c^2} \sin\theta R_{1D}^{(2)}(0) \right|^2 \quad (88)$$

where α is the fine-structure constant and e_c the charm electric charge. A similar expression holds for $\psi(4415)$ and $\psi(4166)$. If the QCD corrections are identical for the two states it comes

$$\begin{aligned} \frac{M^2[\psi(3770)] \Gamma_{e^+e^-}(\psi(3770))}{M^2[\psi(2S)] \Gamma_{e^+e^-}(\psi(2S))} &= \frac{\left| \frac{0.917 \sin\theta + 0.1095 \cos\theta}{0.917 \cos\theta - 0.1095 \sin\theta} \right|^2}{=} \\ &= 0.1295 \pm 0.021 \end{aligned} \quad (89)$$

$$\begin{aligned} \frac{M^2[\psi(4415)] \Gamma_{e^+e^-}(\psi(4415))}{M^2[\psi(4160)] \Gamma_{e^+e^-}(\psi(4160))} &= \frac{\left| \frac{0.944 \sin\theta' + 0.202 \cos\theta'}{0.944 \cos\theta' - 0.202 \sin\theta'} \right|^2}{=} \\ &= 0.688 \pm 0.25. \end{aligned} \quad (90)$$

Fitting these ratios yields the solutions $\theta = 13^\circ \pm 1.5^\circ$, $-26.6^\circ \pm 1.5^\circ$ and $\theta' = 27.6^\circ \pm 5.2^\circ$, $-51.8^\circ \pm 5.2^\circ$ and the semileptonic decay widths become

	$\Gamma_{e^+e^-}$ no mixing	$\Gamma_{e^+e^-}$ with mixing	$\Gamma_{e^+e^-}$ exp
$\psi(2S)$	3.13	2.83	2.10 ± 0.12
$\psi(3770)$	0.04	0.35	0.26 ± 0.04
$\psi(4160)$	2.49	1.63	0.77 ± 0.23
$\psi(4415)$	0.11	0.99	0.47 ± 0.10

with all widths in keV. Clearly, including the mixing improves the theoretical predictions.

In conclusion, the quark model description of the charmonium spectrum using the potential V_0 is in good agreement with the experimental measurements.

The deviation between the model and the experiment is below 3%. In what concerns the particle decays, V_0 provides the best widths of all quark models for the $1S$ states. In particular, it is able to describe well the two photon widths for $1S$ mesons. Moreover, the total $\eta_c(1S)$ width agrees with the experimental figures by less than two standard deviations, but the $J/\psi(1S)$ differs by roughly a factor of 2. For the remaining states where the comparison was done, V_0 results are in line with the QCD inspired models QCD(BT) and Cornell. Typically, the experimental numbers are within the interval of values reported by the three QCD inspired models.

4.3 Bottomonium

The analysis of the bottomonium spectrum and decays is similar to the charmonium study. The radial wave function and its derivative for various quark models are given in table 7. The Cornell potential produces the largest values for $R^{(l)}(0)$, followed by V_0 . For S wave mesons, with the exception of the lowest mass state, the wave function at the origin is essentially constant for V_0 .

Again, the first requirement for computing the spectrum is the determination of α_s . As before, the strong coupling constant is derived from the $1^3S_1 - 1^1S_0$ mass difference

$$\Delta M(1^3S_3 - 1^1S_1) = \frac{8}{9} \alpha_s \frac{|R_{10}(0)|^2}{m_b^2} = 160 \pm 28 \text{ MeV} \quad (91)$$

where the errors were added in quadrature. For bottomonium $R_{10}(0) = 13.56$ GeV, giving

$$\alpha_s(b\bar{b}) = 0.233 \pm 0.041. \quad (92)$$

The large error in α_s is a result of the poor knowledge of the $\eta_b(1S)$ state. Despite the large errors, $\alpha_s(b\bar{b})$ is compatible within errors with $\alpha_s(c\bar{c}) = 0.2718 \pm 0.0028$. Then, in the calculation of the $b\bar{b}$ properties, we will take for the strong coupling constant the value reported in table 2.

Measuring, in the same way, the strong coupling constant for the other potentials models, it comes

QCD(BT)	Power Law	Log	Cornell
0.66(12)	1.05(18)	0.88(15)	0.34(69).

Despite the large errors, the coupling becomes larger at the bottomonium scale, when compared with the charmonium scale. The exception being the Cornell potential which, similarly to what happens with V_0 , reproduces the same values. In particular, for the power law potential $\alpha_s \sim 1$. Given the large value for α_s , one can question if the approach adopted here (central potential with perturbative corrections) is still applicable to some of the potentials⁸. Apparently, this does not seem to be a problem with V_0 or the Cornell potential.

⁸Of course, alternatively, one could take a different definition for α_s .

For bottomonium, the meson mass was defined as in the charmonium, i.e.

$$M(\text{meson}) = 2m_b + E_{NR} + \Delta_{bb} \quad (93)$$

with $\Delta_{bb} = -1790$ MeV adjusted to reproduce the $\Upsilon(1S)$ mass. The full bottomonium spectrum is reported in table 8. In general, there is good agreement between the theoretical prediction and the measured masses. The deviations of the theoretical value from the experimental number is below the 1% level.

The decays widths for the various mesons, for the set of potentials used in the charmonium, are compared in table 9. See also table 10. Note that the calculation uses the charmonium value for α_s (see table 2). The quark models clearly overestimate the total width by a large factor. The comparison between theory and experiment is must worst for bottomonium than for charmonium. Probably, this is an indication that the factorization $\text{meson} \rightarrow \text{gluons} \rightarrow \text{hadrons}$ is not valid for heavy quarkonium. In what concerns the semileptonic widths, we note the good agreement between the estimates from V_0 potential and the experimental figures for the low mass states. Moreover, if instead of the Particle Data Book numbers, the theoretical numbers from V_0 are compared with the recent CLEO measurements [69], the agreement is improved. Table 9 also shows that the other potentials fail to describe properly both the total width and the semileptonic decays. The exception being the Cornell potential, which produces essentially the same results as V_0 .

The predictions of V_0 for the various bottomonium decays are summarized in tables 10, 11 and 12.

Concerning possible mixing between different states, the theoretical spectrum shows no states with similar quantum numbers and mass differences of ~ 100 MeV. Therefore, at least for the low lying states, it is expected no mixing effects for bottomonium.

The pseudoscalar decay constants can be computed as in the charmonium. Combining the definition given in equation (81) with the results of table 7, it follows

$$f_{\eta(1S)} = \begin{cases} 1182 \text{ MeV} & V_0, \\ 817 \text{ MeV} & \text{QCD(BT)}, \\ 688 \text{ MeV} & \text{Power Law}, \\ 711 \text{ MeV} & \text{Logarithmic}, \\ 1203 \text{ MeV} & \text{Cornell}, \end{cases} \quad (94)$$

for a mass of 9274 MeV. If for charmonium the various theoretical models gave essentially the same results, for bottomonium the predictions differ by almost a factor of two.

4.4 B_c

The description of the charmonium and bottomonium can be extended to the spectrum of $b\bar{c}$ mesons. Note that for the B_c calculation there are no free parameters to adjust, except the overall shift $\Delta_{bc} = -1199$ MeV. The typical velocity, in units of the speed of light, of the quarks in $b\bar{b}$ system is $v \approx 0.1$,

while in charmonium systems $v \approx 0.3$. However, in $b\bar{c}$, due to the unequal quark mass, it follows that $v_c \approx 0.5$ and $v_b \approx 0.04$, i.e. the relativistic corrections are more important to $b\bar{c}$ systems than for charmonium or bottomonium. If this correction is similar for all $b\bar{c}$ mesons, then, hopefully, the computed mass differences are meaningful predictions.

For $b\bar{c}$ mesons, experimentally only the ground state 1S_0 meson was found recently [72]. The new CDF measurement for the meson mass, $6287.0 \pm 4.8 \pm 1.1$ MeV [73], agrees well with the three-flavor lattice QCD calculation which gives $M(B_c) = 6304 \pm 12_{-0}^{+18}$ MeV [74].

For the quark model discussed here, the computation of the meson spectrum follow the same lines as the previous spectra. The mesons are no longer charge conjugate eigenstates and the different L states can mix due to the spin-orbit and tensor interactions. Using the same basis as in the previous calculation and writing

$$V_1 = \langle \vec{L} \cdot \vec{S} \rangle a + \langle \vec{L} \cdot \vec{S}_- \rangle b + \langle S_{12} \rangle c + \langle \vec{s}_c \cdot \vec{s}_b \rangle d, \quad (95)$$

see equations (50), (51), (52), (53), (54) for the definitions of a , b , c and d , where $\vec{S} = \vec{s}_c + \vec{s}_b$ and $\vec{S}_- = \vec{s}_c - \vec{s}_b$, the mass matrix for the P states is given by

$$|M\rangle = \begin{pmatrix} M_0 + a - \frac{2}{5}c & 0 & 0 & 0 \\ 0 & M_0 - a + 2c & -\sqrt{2}b & 0 \\ 0 & -\sqrt{2}b & M_0 & 0 \\ 0 & 0 & 0 & M_0 - 2a - 4c \end{pmatrix} \begin{pmatrix} |^3P_2\rangle \\ |^3P_1\rangle \\ |^1P_1\rangle \\ |^3P_0\rangle \end{pmatrix} \quad (96)$$

and for D states by

$$|M\rangle = \begin{pmatrix} M_0 + 2a - \frac{4}{7}c & 0 & 0 & 0 \\ 0 & M_0 - a + 2c & -\sqrt{6}b & 0 \\ 0 & -\sqrt{6}b & M_0 & 0 \\ 0 & 0 & 0 & M_0 - 3a - 2c \end{pmatrix} \begin{pmatrix} |^3D_3\rangle \\ |^3D_2\rangle \\ |^1D_2\rangle \\ |^3D_1\rangle \end{pmatrix}. \quad (97)$$

In (96) and (97) M_0 is the associated central potential eigenvalue.

The $b\bar{c}$ wave function and its derivatives at the origin for various quark models are reported in table 13

As before, the meson mass is defined as

$$M = m_b + m_c + E_{NR} + \Delta_{bc}. \quad (98)$$

The Δ_{bc} is adjusted to reproduce the only experimental $b\bar{c}$ state. In the calculation of the spin splittings, the value used for α_s is the charmonium figure. Various quark model predictions, together with lattice predictions, for B_c mesons are reported in table 14.

In table 13, the various $|R(0)|^2$ are reported for B_c S wave mesons. As before, one can use the values of table 13 to compute the pseudoscalar decay constants. The theoretical estimates can be seen in table 15.

5 Results and Conclusions

In this paper it is proposed an ansatz for the gluon field which is a generalization of the Faddeev-Niemi ansatz - see equations (9), (20) and (21). The gluon field is written in terms of two vector fields and a real scalar field in the adjoint representation of SU(3). In its simplest parameterization, A_μ is given by (26) and the associated classical equations of motion become abelian-like equations. Moreover, the hamiltonian and spin tensor are the sum of two abelian-like contributions from the two vector fields. In Landau gauge, the solutions of the classical equations of motion can be written as plane waves, with a time-like four momenta, and with the A_μ having longitudinal and transverse polarizations. A particular class of solutions with zero classical energy is built. These configurations are asymptotically growing exponential functions in space and in time and are characterized by a unique mass scale. From these solutions, a potential for heavy quark phenomenology is suggested and investigated. In the range of 0.2 - 1 fm, the new potential follows essentially the singlet potential but differs from it for small and large inter-quark separations. The minimization of the square difference between the potentials gives $\Lambda = 228.0$ MeV for the energy scale of the classical solutions.

The potential, including perturbatively the spin dependent contributions, is then used to investigate $c\bar{c}$, $b\bar{b}$ and $b\bar{c}$ mesons. In what concerns the mass spectra, the description is precise up to 3% level for charmonium and below the 1% level for bottomonium. A first study of the mesons decays was performed, comparing the results from the new potential to standard potentials used in heavy quarkonium. In what concerns the hadronic decays, all potentials give, in general, a quite poor description, being able to reproduce the order of magnitude of the particles total width. Typically, the theoretical prediction of the total width overestimates (charmonium) or underestimates (bottomonium) the observed value. In what concerns the semileptonic decays of S wave mesons, the new potential is in line with the others potential model calculations for charmonium. However, for bottomonium the widths computed with the new potential are in good agreement with the recent CLEO measurements.

The calculation of the various spectrum and decays suggest that the potential and, hopefully, the classical configurations discussed here can teach us something about heavy quarkonium. At minimum, the results from the new potential are complementary to the usual quark models for heavy quarkonium. The results discussed here are encouraging and they seem to provide a good starting point for a more elaborated calculation. Within the approach adopted, i.e. a central potential which resumes the non-perturbative physics and the spin effects included in perturbation theory, it remains to be done a coupled channel calculation, including possible effects from exotic contributions (glueballs, $\bar{q}qg$

states, etc.). We are currently engaged in performing such analysis, not only the spectrum determination but also a detailed calculation of the decays of the various states. Moreover, it also remains to estimate the importance of the various multipoles of our solution to heavy quarkonium.

Acknowledgements

R. A. Coimbra acknowledges financial support from Fundação para Ciência e Tecnologia, grant BD/8736/2002.

References

- [1] K. Wilson, Phys. Rev. **D10** (1974) 2445.
- [2] G. S. Bali, Phys. Rep. **343** (2001) 1 [hep-ph/0001312].
- [3] G. S. Bali, K. Schilling, Phys. Rev. **D47** (1993) 661 [hep-lat/9208028].
- [4] S. Necco, hep-lat/0306005.
- [5] Y. Nambu, Phys. Rev. **D10** (1974) 4662.
- [6] G. 't Hooft, in Proceedings of the EPS International Conference, edited by A. Zichichi, p. 1225 (1976).
- [7] S. Mandelstam, Phys. Rep. **23C** (1976) 245.
- [8] T. Suzuki, K. Ishiguro, Y. Mori, T. Sekido, Phys. Rev. Lett. **94** (2005) 132001 [hep-lat/0410001].
- [9] G. 't Hooft, Nucl. Phys. **B138** (1978) 1.
- [10] J. M. Cornwall Nucl. Phys. **B157** (1979) 392.
- [11] H. B. Nielsen, P. Olesen, Nucl. Phys. **B160** (1979) 380.
- [12] L. Del Debbio, M. Faber, J. Greensite, Š. Olejnik, Phys. Rev. **D55** (1997) 2298.
- [13] M. Quandt, H. Reinhardt, M. Engelhardt, PoS(LAT2005)320 [hep-lat/0509114].
- [14] See, for example, J. F. Donoghue, E. Golowich, B. R. Holstein, T. Ericson, *Dynamics of the Standard Model*, CUP 1994, and references therein.
- [15] J. Richardson, Phys. Lett. **B82** (1979) 272.
- [16] W. Buchmüller, S.-H. H. Tye, Phys. Rev. **D24** (1981) 132.
- [17] A. Martin Phys. Lett. **B93** (1980) 338.

- [18] C. Quigg, J. L. Rosner, Phys. Lett. **B71** (1977) 153.
- [19] E. Eichten, K. Gottfried, T. Kinoshita, K. D. Lane, T.-M. Yan, Phys. Rev. **D17** (1978) 3090; **D21** (1978) 313(E); **D21** (1980) 203.
- [20] O. Oliveira, R. A. Coimbra, hep-ph/0305305.
- [21] O. Oliveira, Aip Conf. Proc, **756** (2005) 375.
- [22] K. Huang, *Quarks, Leptons & Gauge Fields*, World Scientific, 1992.
- [23] Y. M. Cho, Phys. Rev. **D62** (2000) 074009.
- [24] L. Faddeev, A. J. Niemi, Phys. Lett. **B464** (1999) 90.
- [25] E. J. Eichten, C. Quigg, Phys. Rev. **D49** (1994) 5845.
- [26] D. Gromes, *Z. Phys.* **C26** (1984) 401.
- [27] S. Eidelman *et al.*, Phys. Lett. **B592** (2004) 1 and 2005 partial update for the 2006 edition available on the PDF WWW pages.
- [28] E. J. Eichten, C. Quigg, Phys. Rev. **D52** (1995) 1726.
- [29] See K. K. Seth hep-ex/0501152 and references therein.
- [30] K. Abe *et al.* (Belle Collaboration), hep-ex/0505037.
- [31] K. Abe *et al.* (Belle Collaboration), hep-ex/0505038.
- [32] K. Abe *et al.* (Belle Collaboration), hep-ex/0507033.
- [33] K. Abe *et al.* (Belle Collaboration), hep-ex/0507019.
- [34] B. Aubert *et al.* (Babar Collaboration), Phys. Rev. Lett. **95** (2005) 142001 [hep-ex/0507090].
- [35] J. L. Rosner *et al.* (Cleo Collaboration), Phys. Rev. Lett. **95** (2005) 102003 [hep-ex/0505073].
- [36] K. K. Seth (CLEO Collaboration) hep-ex/0504050.
- [37] S.-K. Choi *et al.* (Belle Collaboration), Phys. Rev. Lett. **89** (2002) 102001; Err. *ibid*, Phys. Rev. Lett. **89** (2002) 129901 [hep-ex/0206002].
- [38] K. Abe *et al.* (Belle Collaboration), Phys. Rev. Lett. **89** (2002) 142001.
- [39] D. M. Asner *et al.* (CLEO Collaboration), Phys. Rev. Lett. **92** (2004) 142001 [hep-ex/0312058].
- [40] B. Aubert *et al.* (BaBar Collaboration), Phys. Rev. Lett. **92** (2004) 142002 [hep-ex/0311038].

- [41] K. Todyshev *et al.* (KEDR Collaboration), to appear in proceedings of the HEP2005, July 2005, Lisbon, Portugal.
- [42] F. Porter, in *Proceedings of the 17th Rencontre de Moriond Workshop on New Flavors*, Les Arcs, France, 1982, p. 27, (SLAC Report No. SLAC-PUB-2895).
- [43] E. D. Bloom, C. W. Peck, *Annu. Rev. Nucl. Part. Sci.* **33** (1983) 143.
- [44] T. A. Armstrong *et al.* (E760 Collaboration), *Phys. Rev. Lett.* **69** (1992) 2337.
- [45] C. Edwards *et al.* (Cristal Ball Collaboration), *Phys. Rev. Lett.* **48** (1982) 70.
- [46] M. Okamoto *et al.* (CP-PACS Collaboration), *Phys. Rev.* **D65** (2002) 094508.
- [47] L. Antoniazzi *et al.* (E705 Collaboration), *Phys. Rev.* **D50** (1994) 4258.
- [48] J. Z. Bai *et al.* (BES Collaboration), *Phys. Rev.* **D57** (1998) 3854.
- [49] S. -K. Choi *et al.* (Belle Collaboration), *Phys. Rev. Lett.* **91** (2003) 262001.
- [50] D. Acosta *et al.* (CDF Collaboration), *Phys. Rev. Lett.* **93** (2004) 072001.
- [51] V. M. Abazov *et al.* (D0 Collaboration), *Phys. Rev. Lett.* **93** (2004) 162002.
- [52] B. Aubert *et al.* (BABAR Collaboration), *Phys. Rev.* **D71** (2005) 071103.
- [53] N. E. Adam *et al.* (CLEO Collaboration), hep-ex/0508023.
- [54] See E. Swanson, hep-ph/0509237 and references therein.
- [55] See C. Quigg *PoS (HEP2005)* 400 [hep-ph/0509332] and references therein.
- [56] See T. Lesiak hep-ex/0511003 and references therein.
- [57] S. -K. Choi *et al.* (Belle Collaboration), *Phys. Rev. Lett.* **94** (2005) 182002.
- [58] Z. Li *et al.* (CLEO Collaboration), *Phys. Rev.* **D71** (2005) 111103(R).
- [59] D. H. Miller, *Recent charmonium results from CLEO*, talk given at HEP2005, July 2005, Lisbon, Portugal.
- [60] See [27] and references therein.
- [61] R. van Royen, V. F. Weisskopf, *Nuovo Cimento* **50** (1967) 617; **51** (1967) 583.
- [62] See [63], [64] and [65] for the expressions for the various decay widths, including QCD corrections.

- [63] W. Kwong, J. L. Rosner, *Ann. Rev. Nucl. Part. Sci.* **37** (1987) 325.
- [64] W. Kwong, P. B. Mackenzie, R. Rosenfeld, J. L. Rosner, *Phys. Rev.* **D37** (1988) 3210.
- [65] L. Köpke, N. Wermes, *Phys. Rep.* **174** (1989) 67.
- [66] G. S. Adams *et al.* (CLEO Collaboration), hep-ex/0512046.
- [67] J. L. Rosner, *Phys. Rev.* **D64** (2001) 094002.
- [68] V. A. Novikov *et al.*, *Phys. Rep.* **41C** (1978) 1.
- [69] J. E. Dubosq (CLEO Collaboration), hep-rx/061036.
- [70] S. Dobbs *et al.* (CLEO Collaboration), hep-ex/0510033.
- [71] K. K. Seth (CLEO Collaboration), hep-ex/0512039.
- [72] F. Abe *et al.* (CDF Collaboration), *Phys. Rev. Lett.* **81**, 2432 (1998).
- [73] D. Acosta *et al.* (CDF Collaboration), hep-ex/0505076.
- [74] I. F. Allison *et al.* (HPQCD, Fermilab Lattice, UKQCD Collaborations), *Phys. Rev. Lett.* **94** (2005) 172001 [hep-lat/0411027].
- [75] S. Godfrey and N. Isgur, *Phys. Rev.* **D32** (1985) 189.
- [76] D. Ebert, R. N. Faustov, V. O. Galkin, *Phys. Rev.* **D67** (2003) 014027 (2003) [arXiv:hep-ph/0210381].
- [77] L. P. Fulcher, *Phys. Rev.* **D60** (1999) 074006 [arXiv:hep-ph/9806444].
- [78] S. S. Gershtein, V. V. Kiselev, A. K. Likhoded, A. V. Tkabladze, *Phys. Rev.* **D51** (1995) 3613 [arXiv:hep-ph/9406339].
- [79] S. N. Gupta, J. M. Johnson, *Phys. Rev.* **D53** (1996) 312 [arXiv:hep-ph/9511267].
- [80] J. Zeng, J. W. Van Orden, W. Roberts, *Phys. Rev.* **D52** (1995) 5229 [arXiv:hep-ph/9412269].
- [81] N. Brambilla *et al.*, *Heavy Quarkonium Physics*, hep-ph/0412158.
- [82] B. D. Jones, R. M. Woloshyn, *Phys. Rev.* **D60** (1999) 014502.

state	Theory	Particle	Experiment.	deviation
1^3S_1	3097*	$J/\psi(1S)$	3096.916 ± 0.011	
1^1S_0	2980*	$\eta_c(1S)$	2980.4 ± 1.2	
1^3P_2	3483	$\chi_{c2}(1P)$	3556.26 ± 0.11	2.1%
1^3P_1	3481	$\chi_{c1}(1P)$	3510.59 ± 0.10	0.8%
1^3P_0	3451	$\chi_{c0}(1P)$	3415.16 ± 0.35	1.0%
1^1P_1	3479	$h_c(1P)$	$3524.4 \pm 0.6 \pm 0.4$	1.3%
2^3S_1	3699	$\psi(2S)$	3686.093 ± 0.034	0.4%
2^1S_0	3599	$\eta'_c(2S)$	3637.4 ± 4.4	1.1%
1^3D_3	3772			
1^3D_2	3793	$\psi(3836)$	3836 ± 13	1.1%
1^3D_1	3799	$\psi(3770)$	$3773.5 \pm 0.9 \pm 0.6$	0.7%
1^1D_2	3784	$X(3872)$	$3872 \pm 0.6 \pm 0.5$	2.2%
2^3P_2	4037	$Z(3930)$	$3931 \pm 4 \pm 2$	2.7%
2^3P_1	4030			
2^3P_0	3991	$X(3940)$	3936 ± 0.014	1.4%
2^1P_1	4029			
1^3F_4	4044			
1^3F_3	4082			
1^3F_2	4106			
1^1F_3	4071			
3^3S_1	4274	$Y(4260)$	4260	0.3%
3^1S_0	4168			
2^3D_3	4324			
2^3D_2	4344			
2^3D_1	4348			
2^1D_2	4335			
3^3P_2	4604			
3^3P_1	4593			
3^3P_0	4544			
3^1P_1	4593			
2^3F_4	4602			
2^3F_3	4640			
2^3F_2	4663			
2^1F_3	4629			
4^3S_1	4857			
4^1S_0	4742			
3^3D_3	4894			
3^3D_2	4912			
3^3D_1	4914			
3^1D_2	4904			

Table 3: Charmonium spectrum up to 5000 MeV. The table includes only $L \leq 4$ states. The quantum states with * where used to set the model parameters (m_c , α_s , Δ_{cc}).

	V_0	QCD (BT)	Power Law	Log	Cornell	Exp.
$\eta_c(1S)$						
$\rightarrow \gamma\gamma$ (keV)	9.8	7.0	7.6	6.9	13.7	$7.0^{+1.0}_{-0.9}$
$\rightarrow gg$ (MeV)	30.7	48.9	91.9	52.4	61.8	25.5 ± 3.4
$J/\psi(1S)$						
$\rightarrow l^+l^-$ (keV)	5.21	3.11	2.66	2.99	6.80	5.40 ± 0.17
$\rightarrow ggg$ (keV)	190	310	559	332	392	91.0 ± 3.2
$\rightarrow gg\gamma$ (keV)	10.1	8.11	5.1	7.8	15.8	
$\eta_c^l(2S)$						
$\rightarrow \gamma\gamma$ (keV)	5.8	3.1	2.9	2.4	5.9	1.3 ± 0.6
$\rightarrow gg$ (MeV)	18.1	21.4	34.5	18.0	26.5	$< 14 \pm 7$
$\psi(2S)$						
$\rightarrow l^+l^-$ (keV)	3.13	1.43	1.05	1.08	3.06	2.12 ± 0.16
$\rightarrow ggg$ (keV)	115	143	221	120	176	281 ± 17
$\rightarrow gg\gamma$ (keV)	6.1	3.7	2.0	2.8	7.1	
$\psi(4040)$						
$\rightarrow l^+l^-$ (keV)	2.49	1.03	0.64	0.62	2.17	0.75 ± 0.15
$\rightarrow ggg$ (MeV)	0.091	0.102	0.135	0.069	0.125	52 ± 10
$\rightarrow gg\gamma$ (keV)	4.84	2.68	1.23	1.61	5.04	
$\psi(4160)$						
$\rightarrow l^+l^-$ (keV)	2.49	0.96	0.61	0.58	2.05	0.77 ± 0.23
$\rightarrow ggg$ (MeV)	0.091	0.097	0.127	0.065	0.118	78 ± 20
$\rightarrow gg\gamma$ (keV)	4.84	2.53	1.16	1.52	4.75	

Table 4: Charmonium decay widths. The full expressions used for the various decays widths were taken from [63], assuming a quark mass $m_Q = M/2$, where M is the meson mass. In the calculation of the widths, for V_0 it was used the model prediction for M (see table 3), while for the other models it was used the experimental value reported in the Particle Data Book. The referred experimental pure gluonic width is the experimental particle width.

	V_0	$V_0 + \text{QCD}$	exp.
$\eta_c(1S)$			
$\rightarrow \gamma\gamma$ (keV)	13.9	9.8	$7.0^{+1.0}_{-0.9}$
$\rightarrow gg$ (MeV)	21.7	30.7	25.5 ± 3.4
$J/\Psi(1S)$			
$\rightarrow l^+l^-$ (keV)	9.67	5.21	$5.40 \pm 0.15 \pm 0.07$
$\rightarrow ggg$ (keV)	280	190	91.0 ± 3.2
$\rightarrow gg\gamma$ (keV)	24.1	10.1	
$\eta'_c(2S)$			
$\rightarrow \gamma\gamma$ (keV)	8.2	5.8	1.3 ± 0.6
$\rightarrow gg$ (MeV)	12.8	18.1	14 ± 7
$\Psi(2S)$			
$\rightarrow l^+l^-$ (keV)	5.82	3.13	2.12 ± 0.16
$\rightarrow ggg$ (keV)	169	115	281 ± 17
$\rightarrow gg\gamma$ (keV)	14.5	6.1	
$\eta_c(3S)$			
$\rightarrow \gamma\gamma$ (keV)	6.48	4.57	
$\rightarrow gg$ (MeV)	10.1	14.3	
$\Psi(3S)$			
$\rightarrow l^+l^-$ (keV)	4.62	2.49	
$\rightarrow ggg$ (keV)	134	91	
$\rightarrow gg\gamma$ (keV)	11.5	4.84	
$\eta_c(4S)$			
$\rightarrow \gamma\gamma$ (keV)	5.40	3.81	
$\rightarrow gg$ (MeV)	8.4	11.9	
$\Psi(4S)$			
$\rightarrow l^+l^-$ (keV)	3.86	2.08	
$\rightarrow ggg$ (keV)	112	76.1	
$\rightarrow gg\gamma$ (keV)	9.62	4.04	
$\chi_{c2}(1P)$			
$\rightarrow \gamma\gamma$ (keV)	0.552	0.297	0.559 ± 83
$\rightarrow gg$ (MeV)	0.862	0.698	1.55 ± 0.11
$\chi_{c1}(1P)$			
$\rightarrow q\bar{q} + \text{glue}$ (keV)	82.08	–	$0.91 \pm 0.13 \text{ MeV}$
$\chi_{c0}(1P)$			
$\rightarrow \gamma\gamma$ (keV)	2.15	2.19	2.62 ± 0.55
$\rightarrow gg$ (MeV)	3.35	6.11	10.1 ± 0.8
$h_c(1P_1)$			
$\rightarrow \text{glue}$ (keV)	158.0	–	$< 1.1 \text{ MeV}$

Table 5: V_0 decay widths for charmonium. The table shows the widths before including QCD corrections (V_0) and with QCD corrections ($V_0 + \text{QCD}$). The widths were computed according to [68]. The pure gluonic experimental number refers to the total particle width. For $\chi_{c2}(1P)$ the semileptonic width was taken from [70] and the total width from [71].

	$ R_{nl}^{(l)}(0) ^2$	Γ_{theo}	assign.	Γ_{exp}
1^3S_1	0.872 GeV ³	4.64	J/ψ	$5.40 \pm 0.15 \pm 0.07$
2^3S_1	0.773 GeV ³	2.87	$\psi(2S)$	2.14 ± 0.21
3^3S_1	0.827 GeV ³	2.28	$\psi(4040)$	0.75 ± 0.15
			$\psi(4160)$	0.77 ± 0.23
4^3S_1	0.897 GeV ³	1.90	$\psi(4415)$	0.47 ± 0.10
1^3D_1	0.014 GeV ⁷	0.046	$\psi(3770)$	0.24 ± 0.05
2^3D_1	0.047 GeV ⁷	0.22	$\psi(4160)$	0.77 ± 0.23
			$\psi(4415)$	0.47 ± 0.10

Table 6: Squared radial wave function and its derivatives at the origin for charmonium. The semileptonic widths are in keV. The experimental numbers are from the Particle Data Book. New measurements for the $\Gamma_{e^+e^-}$ have been reported by the CLEO collaboration at HEP2005 [58, 59].

	V_0	QCD(BT)	$ R_{nl}^{(l)}(0) ^2$	Power law	Logarithmic	Cornell
1S	13.56	6.477	4.591	4.916	14.05	
2S	4.783	3.234	2.571	2.532	5.668	
3S	4.264	2.474	1.858	1.736	4.271	
4S	4.186	2.146	1.471	1.324	3.663	
5S	4.219	1.956	1.231	1.077	3.319	
2P	1.638	1.417	1.572	1.535	2.067	
3P	2.249	1.653	1.660	1.513	2.440	
4P	2.909	1.794	1.593	1.377	2.700	
5P	3.621	1.935	1.504	1.252	2.917	
3D	1.737	0.637	0.892	0.765	0.860	
4D	2.920	1.191	1.396	1.119	1.636	
5D	4.478	1.722	1.689	1.289	2.417	

Table 7: Bottomonium radial wave function and its derivatives at the origin. All quantities are in GeV^{2l+3}. The first column reports the value computed using $V_0(r)$ and all others are taken from [28]. The references for the various potentials are: QCD(BT) [16], Power law [17], Logarithmic [18], Cornell [19].

state	Theor.	Particle	Experiment	deviation
1^3S_1	9.460*	$\Upsilon(1S)$	9.46030 ± 0.00026	
1^1S_0	9.274	$\eta_b(1S)$	$9300 \pm 20 \pm 20$	0.28%
1^3P_2	9.919	$\chi_{b2}(1P)$	$9.91221 \pm 0.00026 \pm 0.00031$	0.07%
1^3P_1	9.910	$\chi_{b1}(1P)$	$9.89278 \pm 0.00026 \pm 0.00031$	0.17%
1^3P_0	9.892	$\chi_{b0}(1P)$	$9.85944 \pm 0.00042 \pm 0.00031$	0.33%
1^1P_1	9.913			
2^3S_1	9.993	$\Upsilon(2S)$	10.02326 ± 0.00031	0.30%
2^1S_0	9.928			
1^3D_3	10.141	$\Upsilon(1D)$	$10.1611 \pm 0.6 \pm 1.6$	0.21%
1^3D_2	10.140			
1^3D_1	10.137			
1^1D_2	10.140			
2^3P_2	10.261	$\chi_{b2}(2P)$	$10.26855 \pm 0.00022 \pm 0.00050$	0.07%
2^3P_1	10.252	$\chi_{b1}(2P)$	$10.25546 \pm 0.00022 \pm 0.00050$	0.03%
2^3P_0	10.233	$\chi_{b0}(2P)$	$10.2325 \pm 0.0004 \pm 0.0005$	0.00%
2^1P_1	10.255			
1^3F_4	10.324			
1^3F_3	10.327			
1^3F_2	10.327			
1^3F_3	10.326			
3^3S_1	10.353	$\Upsilon(3S)$	10.3552 ± 0.0005	0.2%
3^1S_0	10.294			
2^3D_3	10.461			
2^3D_2	10.460			
2^3D_1	10.457			
2^1D_2	10.460			
3^3P_2	10.591			
3^3P_1	10.581			
3^3P_0	10.561			
3^1P_1	10.584			
2^3F_4	10.642			
2^3F_3	10.643			
2^3F_2	10.643			
2^3F_3	10.643			
4^3S_1	10.694	$\Upsilon(4S)$	10.5800 ± 0.0035	1.08%
4^1S_0	10.636			
3^3D_3	10.784	$\Psi(10860)$	10.865 ± 0.008	0.80%
3^3D_2	10.783			
3^3D_1	10.778			
3^1D_2	10.783			
3^3F_4	10.964			
3^3F_3	10.965			
3^3F_2	10.965			
3^3F_3	10.964			
4^3P_2	10.920		33	
4^3P_1	10.910			
4^3P_0	10.888			
4^1P_1	10.913			
5^3S_1	11.032	$\Psi(11020)$	11.019 ± 0.008	0.12%
5^1S_0	10.974			
4^3D_3	11.111			
4^3D_2	11.109			
4^3D_1	11.104			
4^1D_2	11.109			

	V_0	QCD (BT)	Power law	Logarithmic	Cornell	exp.
$\Upsilon(1S)$						
$\rightarrow l^+l^-$ (keV)	1.93	0.67	0.33	0.48	1.75	1.314 ± 0.029
$\rightarrow ggg$ (keV)	239.6	202.2	183.5	160.9	329.1	53.0 ± 1.5
$\rightarrow gg\gamma$ (keV)	3.21	1.14	7.57	0.77	3.24	
$\Upsilon(2S)$						
$\rightarrow l^+l^-$ (keV)	0.610	0.296	0.164	0.222	0.633	0.587 ± 0.025
$\rightarrow ggg$ (keV)	75.7	90.0	91.6	73.8	118.7	30.6 ± 2.3
$\rightarrow gg\gamma$ (keV)	1.02	0.51	3.78	0.35	1.17	
$\Upsilon(3S)$						
$\rightarrow l^+l^-$ (keV)	0.507	0.212	0.111	0.142	0.447	0.481 ± 0.075
$\rightarrow ggg$ (keV)	62.9	64.5	62.0	47.4	83.8	22.1 ± 2.7
$\rightarrow gg\gamma$ (keV)	0.84	0.36	25.6	0.23	0.82	
$\Upsilon(4S)$						
$\rightarrow l^+l^-$ (keV)	0.467	0.176	0.084	0.104	0.367	0.248 ± 0.031
$\rightarrow ggg$ (keV)	57.9	53.6	47.0	34.6	68.8	$20 \pm 2 \pm 4$
$\rightarrow gg\gamma$ (keV)	0.78	0.30	1.94	0.17	0.68	

Table 9: Mesons decay widths predictions from the various quark model for bottomonium, computed according to [68]. The experimental numbers are from the PDG [27]. In what concerns the semileptonic width, recent measurements from CLEO [69] give $\Gamma_{ee}(1S) = 1.336 \pm 0.009 \pm 0.019$ keV, $\Gamma_{ee}(2S) = 0.616 \pm 0.010 \pm 0.009$ keV, $\Gamma_{ee}(3S) = 0.425 \pm 0.009 \pm 0.006$ keV. The QCD corrections for the power law potential for the process $gg\gamma$ are negative. Therefore, in the table, the results for $gg\gamma$ and for this potential do not include the QCD corrections. The experimental value for the pure gluonic width is the total particle width.

	$ R_{nl}(0) ^2$	Γ_{theo}	Γ_{exp}	CLEO
1^3S_1 [$\Upsilon(1S)$]	13.56	1.934	1.314 ± 0.029	$1.336 \pm 0.009 \pm 0.019$
2^3S_1 [$\Upsilon(2S)$]	4.783	0.611	0.587 ± 0.025	$0.616 \pm 0.010 \pm 0.009$
3^3S_1 [$\Upsilon(3S)$]	4.264	0.508	seen	$0.425 \pm 0.009 \pm 0.006$
4^3S_1 [$\Upsilon(3S)$]	4.186	0.467	0.248 ± 0.031	
5^3S_1 [$\Upsilon(11020)$]	4.219	0.442	0.130 ± 0.030	

Table 10: Square wave function at the origin in GeV^3 and the semileptonic widths in keV for V_0 . The first experimental column are the Particle Data Book results. The second column are the preliminary CLEO results reported at the HEP2005 conference [69].

	V_0	$V_0 + \text{QCD}$	exp.
$\eta_b(1S)$			
$\rightarrow \gamma\gamma$ (keV)	1.24	0.88	
$\rightarrow gg$ (MeV)	31.1	42.9	
$\Upsilon(1S)$			
$\rightarrow l^+l^-$ (keV)	3.59	1.93	1.314 ± 0.029
$\rightarrow ggg$ (keV)	415.9	239.6	53.0 ± 1.5
$\rightarrow gg\gamma$ (keV)	8.93	3.21	
$\eta_b(2S)$			
$\rightarrow \gamma\gamma$ (keV)	0.383	0.270	
$\rightarrow gg$ (MeV)	9.56	13.20	
$\Upsilon(2S)$			
$\rightarrow l^+l^-$ (keV)	1.134	0.610	0.587 ± 0.025
$\rightarrow ggg$ (keV)	131.5	75.7	30.6 ± 2.3
$\rightarrow gg\gamma$ (keV)	2.82	1.02	
$\eta_b(3S)$			
$\rightarrow \gamma\gamma$ (keV)	0.32	0.22	
$\rightarrow gg$ (MeV)	7.93	10.94	
$\Upsilon(3S)$			
$\rightarrow l^+l^-$ (keV)	0.942	0.507	0.481 ± 0.075
$\rightarrow ggg$ (keV)	109.2	62.9	22.1 ± 2.7
$\rightarrow gg\gamma$ (keV)	2.35	0.84	
$\eta_b(4S)$			
$\rightarrow \gamma\gamma$ (keV)	0.29	0.21	
$\rightarrow gg$ (MeV)	7.29	10.1	
$\Upsilon(4S)$			
$\rightarrow l^+l^-$ (keV)	0.867	0.467	0.248 ± 0.031
$\rightarrow ggg$ (MeV)	0.100	0.058	$20 \pm 2 \pm 4$
$\rightarrow gg\gamma$ (keV)	2.16	0.78	
$\eta_b(5S)$			
$\rightarrow \gamma\gamma$ (keV)	0.28	0.20	0.31 ± 0.07
$\rightarrow gg$ (MeV)	6.90	9.53	110 ± 13
$\Upsilon(5S)$			
$\rightarrow l^+l^-$ (keV)	0.820	0.442	0.130 ± 0.030
$\rightarrow ggg$ (MeV)	0.095	0.055	79 ± 16
$\rightarrow gg\gamma$ (keV)	2.04	0.74	

Table 11: V_0 decay widths for bottomonium. The table shows the widths before including QCD corrections (V_0) and with QCD corrections ($V_0 + \text{QCD}$). The widths were computed according to [68]. The pure gluonic experimental number refers to the total particle width. The experimental numbers reported for $Upsilon(4S)$ are the $\Upsilon(10860)$ numbers and for $\Upsilon(5S)$ are the $\Upsilon(11020)$.

	V_0	$V_0 + \text{QCD}$	(a)	exp.
$\chi_{c2}(1P)$				
$\rightarrow \gamma\gamma$ (keV)	0.008	0.005		
$\rightarrow gg$ (MeV)	0.210	0.208		
$\chi_{c1}(1P)$				
$\rightarrow q\bar{q} + \text{glue}$ (keV)	18.5		17.2	
$\chi_{c0}(1P)$				
$\rightarrow \gamma\gamma$ (keV)	0.032	0.032		
$\rightarrow gg$ (MeV)	0.80	1.48		
$h_c(1^1P_1)$				
$\rightarrow \text{glue}$ (keV)	55.3		59.6	
$\chi'_{b2}(2P)$				
$\rightarrow \gamma\gamma$ (keV)	0.011	0.006		
$\rightarrow gg$ (MeV)	0.28	0.30		
$\chi'_{b1}(2P)$				
$\rightarrow q\bar{q} + \text{glue}$ (keV)	20.9		19.4	
$\chi'_{b0}(2P)$				
$\rightarrow \gamma\gamma$ (keV)	0.042	0.043		
$\rightarrow gg$ (MeV)	1.06	1.99		
$h'_b(2^1P_1)$				
$\rightarrow \text{glue}$ (keV)	86.8		93.5	

Table 12: Continuation of table 11.

Level	$ R_{nl}^{(l)}(0) ^2$				
	our	QCD (BT)	Power law	Logarithmic	Cornell
1S	2.333 GeV ³	1.642 GeV ³	1.710 GeV ³	1.508 GeV ³	3.184 GeV ³
2S	1.542 GeV ³	0.983 GeV ³	0.950 GeV ³	0.770 GeV ³	1.764 GeV ³
3S	1.536 GeV ³	0.817 GeV ³	0.680 GeV ³	0.563 GeV ³	1.444 GeV ³
2P	0.324 GeV ⁵	0.201 GeV ⁵	0.327 GeV ⁵	0.239 GeV ⁵	0.342 GeV ⁵
3P	0.506 GeV ⁵	0.264 GeV ⁵	0.352 GeV ⁵	0.239 GeV ⁵	0.461 GeV ⁵
3D	0.300 GeV ⁷	0.055 GeV ⁷	0.101 GeV ⁷	0.055 GeV ⁷	0.102 GeV ⁷

Table 13: Radial wave functions at the origin and related quantities for $b\bar{c}$. The values for the QCD(BT), power law, logarithmic and Cornell potentials are taken from [28].

	V_0	[75]	[76]	[77]	[78]	[25]	[79]	[80]	Lattice [81]
1^3S_1	6380	6338	6332	6341	6317	6337	6308	6340	6321 ± 20
1^1S_0	6286	6271	6270	6286	6253	6264	6247	6260	$6280 \pm 30 \pm 190$
1^3P_2	6768	6768	6762	6772	6743	6747	6773	6760	6783 ± 30
$1P'_1$	6772	6750	6749	6760	6729	6730	6757	6740	6765 ± 30
$1P_1$	6760	6741	6734	6737	6717	6736	6738	6730	6743 ± 30
1^3P_0	6750	6706	6699	6701	6683	6700	6689	6680	6727 ± 30
2^3S_1	6918	6887	6881	6914	6902	6899	6886	6900	6990 ± 80
2^1S_0	6856	6855	6835	6882	6867	6856	6853	6850	6960 ± 80
2^3P_2	7223	7164	7156		7134	7153		7160	
$2P'_1$	7226	7150	7145		7124	7135		7150	
$2P_1$	7214	7145	7126		7113	7142		7140	
2^3P_0	7200	7122	7091		7088	7108		7100	
3^3S_1	7394	7272	7235			7280		7280	
3^1S_0	7332	7250	7193			7244		7240	
1^3D_3	7024	7045	7081	7032	7007	7005		7040	
$1D'_2$	7045	7036	7079	7028	7016	7012		7030	
$1D_2$	7022	7041	7077	7028	7001	7009		7020	
1^3D_1	7040	7028	7072	7019	7008	7012		7010	

Table 14: Theoretical predictions for the $b\bar{c}$ meson spectrum. All masses are in MeV.

	V_0	[76]	QCD(BT)	Power Law	Log	Cornell	[82]
f_{B_c}	595	562	500	512	479	687	420 ± 13
$f_{B_c^*}$	591						

Table 15: Pseudoscalar decay constants of the B_c meson (MeV) for nonrelativistic quark models [76], [25] (BT, power law, logarithmic and Cornell potentials) and lattice NRQCD [82].